frontiers | Frontiers in Marine Science

TYPE Original Research
PUBLISHED 22 June 2023
DOI 10.3389/fmars.2023.1119331

OPEN ACCESS

EDITED BY
Yunyun Zhuang,
Ocean University of China, China

REVIEWED BY
Xiaoshou Liu,
Ocean University of China, China
Huan Zhang,
Chinese Academy of Sciences (CAS), China
Li-Zhe Cai,
Xiamen University, China

*CORRESPONDENCE
Longhui Deng
longhui.deng@sjtu.edu.cn
Mark Alexander Lever
mark.lever@austin.utexas.edu

RECEIVED 08 December 2022
ACCEPTED 09 May 2023
PUBLISHED 22 June 2023

CITATION
Deng L, Fiskal A, Bölsterli D, Meier D, Meile C and Lever MA (2023) Differential impact of two major polychaete guilds on microbial communities in marine sediments: a microcosm study. *Front. Mar. Sci.* 10:1119331. doi: 10.3389/fmars.2023.1119331

Differential impact of two major polychaete guilds on microbial communities in marine sediments: a microcosm study

Longhui Deng[1,2]*, Annika Fiskal[1,3], Damian Bölsterli[1], Dimitri Meier[1], Christof Meile[4] and Mark Alexander Lever[1,5]*

[1]Institute of Biogeochemistry and Pollutant Dynamics, Swiss Federal Institute of Technology, Zurich (ETH Zurich), Zürich, Switzerland, [2]School of Oceanography, Shanghai Jiao Tong University, Shanghai, China, [3]Department of Microbial Ecology, German Federal Institute of Hydrology (BfG), Koblenz, Germany, [4]Department of Marine Sciences, University of Georgia, Athens, GA, United States, [5]Marine Science Institute, University of Texas at Austin, Port Aransas, TX, United States

Even though sediment macrofauna are widespread in the global seafloor, the influence of these fauna on microbial communities that drive sediment biogeochemical cycles remains poorly understood. According to recent field investigations, macrofaunal activities control bacterial and archaeal community structure in surface sediments, but the inferred mechanisms have not been experimentally verified. Here we use laboratory microcosms to investigate how activities of two major polychaete guilds, the lugworms, represented by *Abarenicola pacifica*, and the clamworms, represented by *Nereis vexillosa*, influence microbial communities in coastal sediments. *A. pacifica* treatments show >tenfold increases in microbial cell-specific consumption rates of oxygen and nitrate, largely due to the strong ventilation activity of *A. pacifica*. While ventilation resulted in clearly elevated percentages of nitrifying archaea (*Nitrosopumilus* spp.) in surface sediments, it only minorly affected bacterial community composition. By comparison, reworking – mainly by deposit-feeding of *A. pacifica* – had a more pronounced impact on microorganismal communities, significantly driving down abundances of Bacteria and Archaea. Within the Bacteria, lineages that have been linked to the degradation of microalgal biomass (e.g., Flavobacteriaceae and Rhodobacteraceae), were especially affected, consistent with the previously reported selective feeding of *A. pacifica* on microalgal detritus. In contrast, *N. vexillosa*, which is not a deposit feeder, did not significantly influence microbial abundances or microbial community structure. This species also only had a relatively minor impact on rates of oxygen and nitrogen cycling, presumably because porewater exchanges during burrow ventilation by this species were mainly restricted to sediments immediately surrounding the burrows. Collectively our analyses demonstrate that macrofauna with distinct bioturbation modes differ greatly in their impacts on microbial community structure and microbial metabolism in marine sediments.

KEYWORDS

Bioturbation, animal-microbe interactions, deposit-feeding, sedimentary DNA and RNA, biogeochemical cycles, cell-specific rates, coastal sediment

1 Introduction

Despite covering<1% of Earth's surface area, intertidal and nearshore sediments are globally important hotspots of organic carbon (OC) turnover (Ward et al., 2020). These sediments are among the most productive seafloor ecosystems, supporting high benthic primary production (10^3 to 10^4 mmol C m^2 y^{-1}) and a high biomass of macrofauna (Herman et al., 2001; Cahoon, 2002). Moreover, intertidal and nearshore sediments support high rates of OC decomposition (10^3 to 10^5 mmol C m^2 y^{-1}; Herman et al., 2001; de Beer et al., 2005; Huettel et al., 2014). These rates are orders of magnitude higher than global mean OC decomposition rates for marine surface sediments (~10^1-10^2 mmol C m^2 y^{-1}; LaRowe et al., 2020).

A major part of the OC turnover in intertidal and nearshore sediments is mediated by the activities of burrowing macrofauna (Middelburg, 2018). Through a process called "bioturbation", these macrofauna modify sedimentary matrices and geochemical gradients, thereby altering the zonation and rates of microbial reactions and ultimately the burial of OC (Kristensen et al., 2012). Macrofaunal bioturbation can be categorized into two major processes, termed 'ventilation' and 'reworking' (Kristensen et al., 2012). By ventilating their burrows and surrounding sediments (bioirrigation) with overlying seawater, macrofauna introduce the high-energy electron acceptors dioxygen (O_2) and nitrate (NO_3^-) and stimulate the microbial oxidation of OC in sediment (Aller, 1982). The resulting fluctuations between oxic and anoxic conditions promote coupled nitrification–denitrification reactions (Gilbert et al., 1998). In addition, ventilation increases the oxidative and advective removal of potentially toxic microbial end products, such as reduced metals, sulfide, and ammonium (Thamdrup et al., 1994). By contrast, reworking is defined as the displacement of particles during macrofaunal burrowing, locomotion, and feeding. This introduces labile organic matter and metal oxides to deeper layers and enhances microbial OC cycling in these layers (Aller, 1990; Levin et al., 1997; Middelburg, 2018). Direct feeding by macrofauna also increases OC cycling through the digestive breakdown of biomass and detritus (Plante et al., 1990; Plante and Shriver, 1998) and stimulates microbial growth by supplying more microbially accessible, partially decomposed organic matter (Fenchel, 1970). In addition, macrofaunal secretion of nutrient-rich mucopolysaccharides e.g., for burrow stabilization, can fuel microbial activity (Papaspyrou et al., 2006; Dale et al., 2019).

Despite driving key biogeochemical processes, the impacts of macrofaunal activities on the community structures of sediment microorganisms, which perform most of these processes, are not fully understood. Ventilation of O_2-rich water into burrows has been proposed to explain burrow wall microbial communities distinct from those in surrounding sediment (Marinelli et al., 2002; Satoh et al., 2007; Bertics and Ziebis, 2009) and to also influence microbial communities in surrounding sediment (Mermillod-Blondin et al., 2004; Cuny et al., 2007). Deposit-feeding has been shown to result in selective removal of bacterial taxa during gut passage (Plante and Jumars, 1993; Wilde and Plante, 2002). Recent field studies have, moreover, revealed that the influence of macrofauna on microbial communities extends well past burrow walls and feces and is the most important driver of microbial community structure throughout the entire bioturbated layer (Chen et al., 2017; Deng et al., 2020). While reworking of fresh phytodetritus into deeper layers was proposed to mainly drive bacterial communities, ventilative pumping of seawater-derived electron acceptors was suggested to mainly control archaeal community structure (Deng et al., 2020). More recently, it was hypothesized that selective ingestion of fine, organic-rich particles by the lugworm *Abarencola pacifica* is the dominant driver of microbial community structure in intertidal sediments inhabited by this species, and strongly alters bacterial and eukaryotic, but only to a minor degree archaeal, community networks (Deng et al., 2022).

Despite the results of these recent field investigations, the inferred mechanisms by which macrofaunal activities control bacterial and archaeal community structures in marine sediments have yet to be experimentally verified. Furthermore, it remains unclear how co-occurring polychaete species that differ in bioturbation modes compare in their impacts on microbial communities. Here we use laboratory microcosm experiments involving intertidal sands from False Bay (Washington, USA) to identify mechanisms by which the ecologically and functionally distinct polychaete species *Abarenicola pacifica* and *Nereis vexillosa* influence microbial communities. Both species dominate adjacent parts of the upper intertidal zone of False Bay and are widespread along the coast of the North Pacific (Healy and Wells, 1959; Woodin, 1977), but differ in behavior. *A. pacifica* inhabits a J-shaped burrow and causes intense sediment reworking and bioirrigation through its active subsurface deposit-feeding and seawater-pumping activity (Healy and Wells, 1959; Hylleberg, 1975). By contrast, *N. vexillosa* mainly ventilates its U-shaped burrow and feeds on fauna and algae at the sediment surface (Woodin, 1977).

To investigate how worm behavior impacts sediment biogeochemical processes and microbial communities, we ran 35-day laboratory aquarium experiments in flowing seawater with *A. pacifica* (AP), *N. vexillosa* (NV), and fauna-free controls (Ctrl). We monitored rates of ventilation and reworking, as well as impacts of both processes on porewater geochemical gradients, distributions of labile particulate OC, and turnover rates of dominant electron acceptors and metabolic end products. In parallel, we analyzed DNA and reverse transcribed RNA pools to monitor how microbial abundance, community structure, and activity changed over time and across treatments.

2 Materials and methods

2.1 Study area

Samples were obtained from the False Bay Biological Preserve on San Juan Island, USA, which is owned by the University of Washington (Figure 1A). False Bay is a circular-shaped intertidal embayment (~1 km^2) with mixed semi-diurnal tides (Pamatmat, 1968, Waldbusser and Marinelli 2009). Sediments and macrofauna

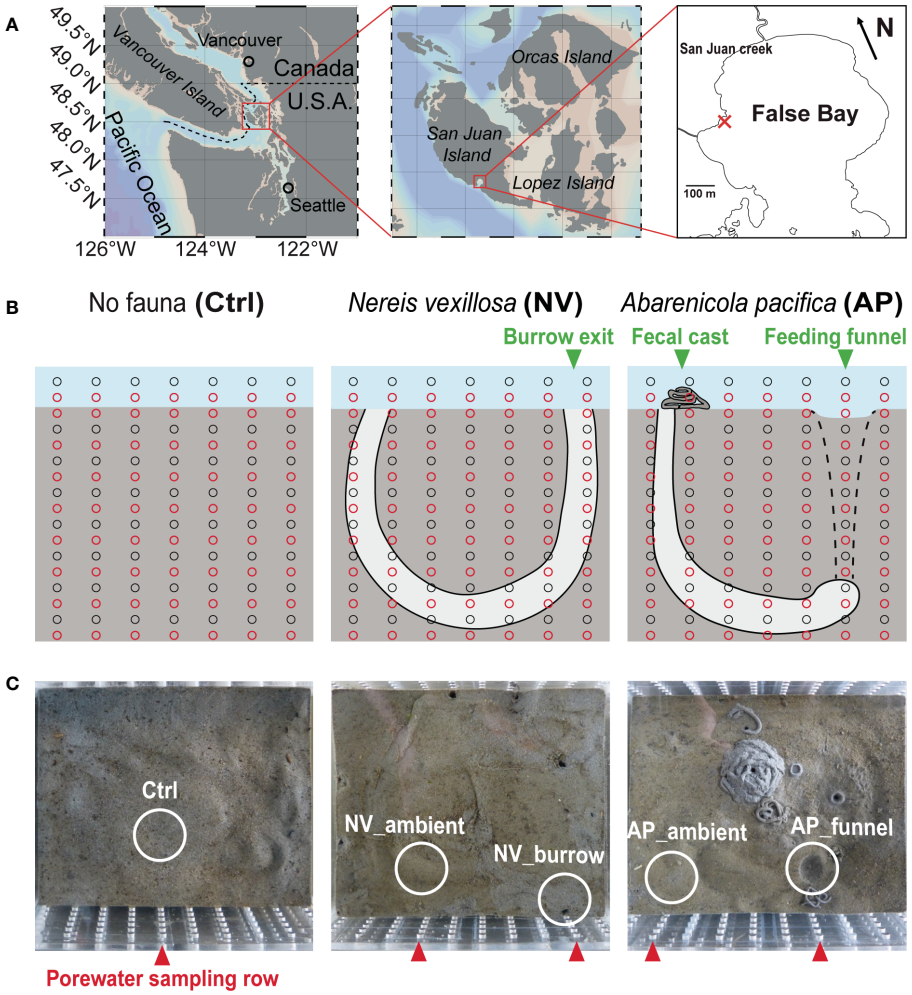

FIGURE 1
Study area and experimental design: **(A)** Maps of study area. The red cross in the right panel denotes the sampling location in False Bay. **(B)** Narrow aquaria: sketch of the three experimental treatments (Ctrl, NV, AP). All porewater and microsensor sampling was performed through predrilled holes (circles). Red circles indicate predrilled holes that were sampled, black circles indicate those holes that were not sampled. **(C)** Wide aquaria: Top view showing sampling scheme of wide aquaria. White circles indicate locations of microsensor measurements, porewater sampling, and sediment core sampling. These locations included Controls (Ctrl), *N. vexillosa* burrow exits (NV_burrow), *A pacifica* feeding funnels (AP_funnel), and locations that were ≥5 cm away from burrow exits or feeding funnels in each worm treatment (NV_ambient, AP_ambient). The red triangles indicate the vertical rows of predrilled holes that were used for porewater sampling using rhizons. As for narrow aquaria, only every second hole was sampled (vertical distance between sampled holes = 2 cm).

were collected from a sandy area that is dominated by *Abarenicola pacifica* and *Nereis* vexillosa (Figure 1A, right panel) and was recently investigated (Deng et al., 2022).

2.2 Macrofaunal species

N. vexillosa lives in a semi-permanent U-shaped burrow (Figure 1B), through which it pumps seawater for respiration, and causes particle mixing over short distances around the burrow ("gallery biodiffusor"). *N. vexillosa* feeds on smaller fauna and green algae (e.g. *Ulvaceae*) outside or at the exit of its burrow (Woodin, 1977). By contrast, *A. pacifica* lives head down in J-shaped burrows (Figure 1B) and causes intense bioirrigation by pumping water through sediment above the burrow end (Hobson, 1967; Hylleberg, 1975). Its main feeding mode consists of the selective ingestion of fine organic-rich particles at the burrow end ("feeding pocket"). Rates of ingestion are often so high that they create a depression at the overlying seafloor ("feeding funnel"). The digested sediments, which are strongly depleted in microalgal, meiofaunal, and microbial biomass (Deng et al., 2022), are expelled back onto the sediment surface as fecal casts ("upward conveyor").

2.3 Experimental design

The impacts of bioturbation by *N. vexillosa* and *A. arenicola* on sediment geochemical conditions and microbial communities was studied experimentally at the Friday Harbor Laboratories for 35 days from July to September 2017 (Figure 1). The three experimental treatments consisted of A. pacifica (AP), N.

vexillosa (NV), and no fauna (Ctrl). Two types of experimental microcosms, called "narrow aquaria" (25×2×20 cm3; L×W×H) and "wide aquaria" (30×25×20 cm3), were built from clear, colorless acrylic (Figure S1A). Narrow aquaria were used for close-up observations of worms and burrow structures. Wide aquaria provided more living space for macrofauna and were thus more representative of the natural setting. In both aquarium types, we analyzed changes in sediment porewater chemistry in response to worm activity. To provide access to sediment porewater from various sediment depths, all aquaria had predrilled holes on the front wall that were plugged with silica gel. These holes were arranged in 7 vertical rows, each spaced 2.5 cm apart. Within each row, individual holes were spaced 1 cm apart. From wide aquaria, we also obtained sediment cores to study reworking activity and its impacts on microbial communities. To sample sediment, we used core liners that were vertically pushed into the sediments at designated locations (see below). All aquaria were filled with sediments that had been sieved through a 1-mm-mesh to remove macrofauna, and carefully homogenized. After sediment addition, aquaria equilibrated under running seawater for 3 days to restore anoxic conditions (confirmed by O_2 microsensor profiling). Experiments were initiated by adding freshly collected adult *A. pacifica* and *N. vexillosa* with body lengths of ~10 cm and ~20 cm, respectively. Wide aquaria received three specimens of *A. pacifica* or *N. vexillosa*, corresponding to 40 specimens m^{-2} (natural density: ~35 *A. pacifica* and ~25 *N. vexillosa* individuals m^{-2}). Narrow aquaria only received a single worm specimen (density: ~200 individuals m^{-2}). Running water consisted of untreated natural seawater from San Juan Channel (O_2 concentration: >200 µM, temperature: 10-13°C, salinity: 20-30). Temperature and salinity were lower than in intertidal sediments of False Bay (temperature: 17-27°C, salinity: 30-33) (Deng et al., 2022). Due to low light intensity, the clear diurnal signal of O_2 production by microphytobenthos in False Bay intertidal sediment was not observed in the laboratory.

Narrow aquaria. We ran two replicates of each treatment (6 aquaria in total) and sampled these destructively after 21 and 35 days (T21 and T35, respectively). Microsensor measurements and porewater sampling was done from the side through the predrilled holes (Figures 1B, S1B). All rows, but only every other hole per row, were analyzed or sampled. This spatial resolution enabled detailed 2D-mapping of how worm activities influence redox potential and porewater solutes.

Wide aquaria. We ran 6 replicates per treatment (18 aquaria in total) and sampled these destructively on five dates, i.e. after 7, 14, 21, 28, and 35 days (T7, T14, T21, T28, and T35, respectively; the sixth replicate was not sampled because of *N. vexillosa* escape from one aquarium). The high number of time points was chosen due to initial uncertainty concerning the time scales over which worms impact sediment geochemistry and microbiology. In the end, we only analyzed the three dates that best represented the entire experimental period, i.e. the first, middle, and final sampling dates (T7, T21, T35). As for narrow aquaria, porewater was sampled from the side through predrilled holes at a depth resolution of 2 cm (Figure 1C). Only the middle row was sampled for control treatments. For worm treatments, two rows were sampled to characterize spatial variations in porewater chemistry in relation to worm activity. One was vertically aligned with an *N. vexillosa* burrow exit (NV_burrow) or *A. pacifica* feeding funnel (AP_feeding funnel). The other row was located ≥5 cm away from the nearest burrow exit or feeding funnel (NV_ambient, AP_ambient) (Figure 1C).

Tracer addition. On day 15 of the experiments, solute- and solid-phase tracers were introduced. Bromide (Br^-) stock solution (5 M) was continuously injected to inflowing seawater using a multi-channel peristaltic pump (final Br^- concentration of overlying water: ~8-10 mM) and used to trace diffusion- and ventilation-induced porewater exchanges with overlying seawater. Luminophores (20 g; 200 µm mean diameter; Environmental Tracing, UK) were evenly spread across the sediment surface to track downward particle mixing by macrofaunal reworking. The chosen diameter was in the same range as the dominant grain size at the sampling site in False Bay (Deng et al., 2022).

2.4 Microsensor profiling

To monitor initial impacts of worm bioturbation on porewater geochemical conditions, we used a micro-profiling system equipped with Clark-type microsensors (Unisense, Denmark).

Narrow aquaria. Redox potential was measured by piercing needle microsensors horizontally through silicon-sealed holes of all 7 vertical rows, going through every second hole. This resulted in a final 2 cm × 2.5 cm grid of data points (see example in Figure S1C).

Wide aquaria. Vertical gradients of dissolved O_2, HS^-, pH, and redox potential in the upper centimeter were monitored using a glass microsensor (tip diameter: 200 µm). In worm treatments, vertical measurements were made at the sediment surface ~0.5 cm from *N. vexillosa* burrow exits (NV_burrow) or inside *A. pacifica* feeding funnels (AP_feeding funnel), and ≥5 cm away from burrow exits or feeding funnels (NV_ambient, AP_ambient; Figure 1C)). In controls, measurements were performed at the center of each aquarium (Ctrl).

2.5 Porewater and sediment sampling

To determine geochemical and microbiological impacts of bioturbation, porewater and sediment were sampled as follows.

Porewater (narrow aquaria). Porewater samples (1.5 mL) from narrow aquaria were obtained by inserting micro-rhizons (0.15 µm pore size, Rhizosphere, Netherlands) immediately after microsensor measurements. For the quantification of inorganic anions, inorganic cations, and hydrogen sulfide (each 0.5 mL), samples were treated as described below for wide aquaria, by adjusting the added volumes of HCl, NaOH, and zinc acetate to account for the smaller sample volumes.

Porewater (wide aquaria). Porewater was extracted by inserting rhizons (0.15 µm pore size, 10 cm porous part, Rhizosphere, Netherlands) through holes on the side at a 2-cm vertical depth resolution. Only the rows that were under the locations of microsensor measurements were sampled (NV_burrow,

AP_feeding funnel, NV_ambient, AP_ambient, Ctrl; Figure 1C). The initial 1-2 mL of porewater were used to flush rhizons and syringes of air, including O_2, and minimize oxidation of redox sensitive solutes, and thus discarded. Afterwards ~12 mL of porewater were withdrawn per depth. For inorganic anion (Br^-, SO_4^{2-}, Cl^-, NO_2^-, NO_3^-) and cation (NH_4^+) analyses, the pH of 3-mL porewater samples was adjusted by adding 5 µL of 2M NaOH or HCl, respectively. Porewater for dissolved Fe^{2+} and Mn^{2+} quantification (3 mL) was fixed with 50 µL of 30% HCl. Samples for the analysis of hydrogen sulfide (1 mL) were fixed with 1 mL of 5% zinc acetate. All porewater samples were stored at 4°C.

Sediment (only wide aquaria). Next, sediments were sampled from the same locations (NV_burrow, AP_feeding funnel, NV_ambient, AP_ambient, Ctrl) by vertically inserting a 4.5 cm diameter core liner to the bottom of aquaria. Sediments were extruded and sampled for solid-phase geochemical and microbiological analyses at 2-cm intervals using sterile cut-off syringes. On T35, we obtained an additional 2 mL of fresh *A. pacifica* fecal piles using a spoon and sediments with mucus from the *N. vexillosa* burrow exit using a 1-mL pipette with cut-off tip, all for microbiological analyses. All sediments were frozen (microbiological samples: -80 °C; geochemical samples: -20 °C).

2.6 Geochemical measurements

Porewater concentrations of Br^-, SO_4^{2-}, and Cl^- were measured by ion chromatography (DIONEX DX-320, details in Fiskal et al., 2019) on 10-fold dilutions. Dissolved Fe^{2+} and Mn^{2+} concentrations were measured by Inductively Coupled Plasma-Optical Emission Spectroscopy (ICP-OES) (5100, Agilent Technologies) with an ICP-multielement standard (solution IV, MERCK, Certipur). A plate reader (Synergy HT, BioTek) was used for photometric quantifications of ammonium (NH_4^+; Solorzano, 1969), nitrate (NO_3^-) and nitrite (NO_2^-) (Miranda et al., 2001), and hydrogen sulfide (HS^-) concentrations (Cline, 1969). Chlorophyll *a* (chl *a*), a proxy for labile organic carbon, was extracted from 1.5 g of wet sediment using acetone (Lever and Valiela, 2005) and quantified spectrophotometrically using an acidification protocol (Cary 50, UV-Vis, Varian; Lorenzen, 1967).

2.7 Nucleic acid analyses

DNA extraction. DNA and RNA were extracted simultaneously from 0.2 g of wet sediments following lysis protocol I of Lever et al. (2015). For details, see Supplementary methods.

Quantitative PCR (qPCR). 16S rRNA genes, reverse transcribed 16S rRNA, and ribulose-1,5-bisphosphate carboxylase genes *(rbc*L) of *Ochrophyta* (mainly diatoms; Deng et al., 2022) were quantified by SYBR-Green I-based qPCR assays using a LightCycler 480 II (Roche Life Science, Switzerland) to evaluate how worms impact abundances of (active) Bacteria and Archaea and labile OC sources (diatoms). For details, see supplementary methods and Table S1.

DNA sequencing and sequence analyses. Library preparations, sequencing, and initial bioinformatic quality controls followed the workflow of Deng et al. (2020). The bacterial and archaeal 16S rRNA gene primers used for amplicon sequencing (MiSeq; 2×250 bp, Illumina Inc., USA) are listed in Table S1. Bacterial 16S genes were taxonomically classified using the SILVA 16S database (release 138.1, Quast et al., 2012). Archaeal 16S genes were assigned in ARB (www.arb-home.de) using neighbor-joining phylogenetic trees that were based on a manually optimized SILVA database that was expanded to include additional 16S gene sequences from whole-genome sequencing studies.

2.8 Rate modeling

Bioirrigation and biogeochemical reaction rates. Bioirrigation rates in wide aquaria were calculated by simulating the measured porewater profiles using the mass conservation equation:

$$\phi \frac{\partial C}{\partial t} = \frac{\partial}{\partial x}\left((D + D_b)\phi \frac{\partial C}{\partial x}\right) + \alpha(x)\phi(C_0(t) - C) + R \quad (1)$$

where C is the concentration of solute, $\phi$is porosity, D and D_b are diffusion coefficients due to molecular diffusion and additional diffusive mixing,$\alpha$is the bioirrigation coefficient, C_0 is the solute concentration in the overlying water at time t, and R is the net reaction rate, set to zero for the nonreactive tracer Br^-. By modeling the Br^- profiles, we first determined the bioirrigation intensity (α= 0 in controls). Net reaction rates of O_2, NO_3^-, SO_4^{2-} and NH_4^+ were then calculated by isolating R in Eq. 1 and approximating the remaining terms from the data (for details, see Supplementary methods).

Rates of particle mixing. Wet sediment (~1.5 g) from all samples from wide aquaria were dried in an oven at 50°C for 6 hrs and homogenized. Three dried aliquots (0.2 g each) were placed in plastic petri dishes and distributed evenly by gentle shaking. Luminophores were counted based on photographs taken using a Sony 6000a digital camera under UV light. The particle mixing index (M_i) was then determined for each layer of sediment:

$$M_i = \left|\frac{L_f - L_c}{L_c'}\right| \times 100 \quad (2)$$

where L_f and L_c are luminophore counts (g^{-1} dw) in faunal and control treatments, respectively.

Cell-specific reaction rates. Cell-specific O_2, NO_3^-, and SO_4^{2-} consumption rates were calculated by dividing O_2, NO_3^-, and SO_4^{2-} consumption rates (see above section "Bioirrigation and biogeochemical reaction rates") by cell numbers of O_2, NO_3^-, and SO_4^{2-} respiring microorganisms by

$$R_{Cell} = \frac{R}{C \times f} \quad (3)$$

where $R$is the reaction rate of O_2, NO_3^-, and SO_4^{2-} calculated based on equation (1), and $C$is the total cell number calculated based on the relationship between 16S gene copies and microscopic cell counts in False Bay sediment (N_{cell} = 0.75*$N_{16S\ gene\ copies}$ -7.7*10^6; Deng et al., 2019). $f$is the fraction of the microbial population that potentially mediates the consumption of O_2 (aerobic heterotrophs, nitrifiers, sulfur and metal oxidizers), NO_3^-

(nitrate reducers), and SO_4^{2-} (sulfate reducers) based on 16S gene functional annotations using FAPROTAX (Louca et al., 2016).

2.9 Statistical analyses

Statistical analyses were performed in R (http://www.R-project.org) and based on ZOTUs unless stated otherwise. Microbial diversity (Shannon index) analysis, PERmutational Multivariate ANalysis Of VAriance (PERMANOVA, 999 permutations), and Partial Mantel Tests were performed using the 'vegan' package (Oksanen et al., 2013). Principal Coordinates Analysis (PCoA) with weighted Unifrac distance was done using the 'phyloseq' package (McMurdie & Holmes, 2013). Boxplots were generated using the 'ggpubr' package. Group-mean values were compared based on Welch's t test with Bonferroni-Holm correction for multiple comparisons using the 'rstatix' package.

3 Results

3.1 Geochemical impacts of worm bioturbation in narrow aquaria

Nereis vexillosa (NV) and *Abarenicola pacifica* (AP) strongly altered the sediment geochemistry as evidenced by 2D maps of Br^-, redox potential, HS^-, and NH_4^+ concentrations after 35 days (T35; Figure 2). Br^- concentrations in controls decreased from ~9 mM at the sediment surface to<1 mM at ~8 cm, but remained at running seawater values in and around worm burrows. While concentrations decreased to<6 mM away from NV burrows, they remained at running water values (~9 mM) throughout AP aquaria. Worm bioturbation also altered the redox potential. In controls, redox decreased from 450 to 50 mV from 0 to 3 cm and ranged from 50 to -150 mV below. In NV aquaria, values remained at 250 to 450 mV along burrows but dropped below 50 mV within 2-3 cm away from burrows. In AP aquaria, redox potentials were highest in the feeding pocket (350 to 550 mV) and within several centimeters of the burrow and feeding funnel (250 to 450 mV), and lowest further away (<50 mV). Reduced end products of sulfate reduction (HS^-) and organic matter mineralization (NH_4^+) showed similar 2D patterns. Both increased to ~2 mM (HS^-) and ~6 mM (NH_4^+) below 5 cm in controls, but were much lower around NV burrows (HS^-:<0.1 mM, NH_4^+:<0.5 mM), and remained below controls away from NV burrows (HS^-: 0.3-0.9 mM, NH_4^+: 0.5-3 mM). In AP aquaria, HS^- and NH_4^+ concentrations were uniformly low (HS^-:<0.1 mM, NH_4^+:<0.5 mM).

3.2 Geochemical impacts of worm bioturbation in wide aquaria

3.2.1 Microsensor gradients

Microsensor profiles in wide aquaria confirmed the strong geochemical impact of both worm species in narrow aquaria (Figure S2). O_2 concentrations decreased below detection within the top 5 mm of all treatments, except feeding funnels of AP where O_2 was measured to 10 mm. HS^- concentrations increased over time in controls (T35: ~30-80 µM) but remained lower in NV (<25 µM) and AP treatments (<10 µM). The pH decreased from ~8 in overlying water to ~7 below 10 mm sediment depth, showing slightly higher values in AP feeding funnels. At T7, redox potential profiles decreased from ~550 mV to ~200 mV in the top 5 mm of all treatments. At later time points they varied considerably but were consistently elevated in feeding funnels of *A. pacifica*.

3.3 Porewater concentration gradients and bioirrigation rates

As in narrow aquaria, AP and NV strongly altered porewater gradients in wide aquaria (Figure 3).

Concentrations of the conservative Br- tracer in Controls decreased with depth and were only detectable to ~5 and ~7 cm at T21 and T35, respectively. By contrast, Br^- concentrations were at 5 to 8 mM throughout NV treatments, with highest values around burrows. In AP treatments, concentrations were at overlying water values throughout the sediments only 6 days after Br^- injection started (T21). Modeling of Br^- profiles suggested approximately 4× higher bioirrigation coefficients in AP (α_{AP} = 0.3-0.8 d^{-1}) than in NV treatments (α_{NV} = 0.12-0.13 d^{-1}, Figure S3).

Impacts of bioturbation were also seen in concentrations of microbial metabolites. NO_3^- concentrations decreased to ~0.1 µM in the upper 3 cm, except in AP feeding funnels and NV burrows, where concentrations remained elevated (0.5-2 µM). NH_4^+ concentrations increased with depth and incubation time in controls (to 11 mM) and NV treatments (to 8 mM), but remained much lower (<0.7 mM) throughout AP aquaria.

SO_4^{2-} concentrations were >22 mM throughout all wide aquaria (seawater: ~24-25 mM). In controls, values decreased to 22-23 mM at 5-9 cm sediment depth, but increased back to ~24 mM below. In contrast, SO_4^{2-} concentrations remained near seawater values throughout AP treatments, and were also lower in NV treatments compared to controls. HS^- concentrations were low at T7 and T21 but increased to ~0.3 mM in controls and to ~0.2-0.8 mM in NV treatments at T35. By contrast, HS^- concentrations were consistently<0.1 mM in AP treatments throughout the experiments.

Fe^{2+} concentrations increased initially in controls and NV treatments, from presumably zero during the oxic onset of incubations to ~200 µM in controls and ~90 µM in NV treatments at T7, but returned to low concentrations at T35 likely due to precipitation with HS^-. By contrast, Fe^{2+} concentrations remained below<20 µM independent of depth or incubation time in AP treatments.

3.3.1 Particle mixing and indices of feeding activity

Luminophores, which were added 15 days after the onset of incubations, were only detectable in the topmost layer (~1 cm) of controls at T21 and T35, consistent with the absence of macrofaunal sediment mixing (Figure 4). In NV and AP treatments,

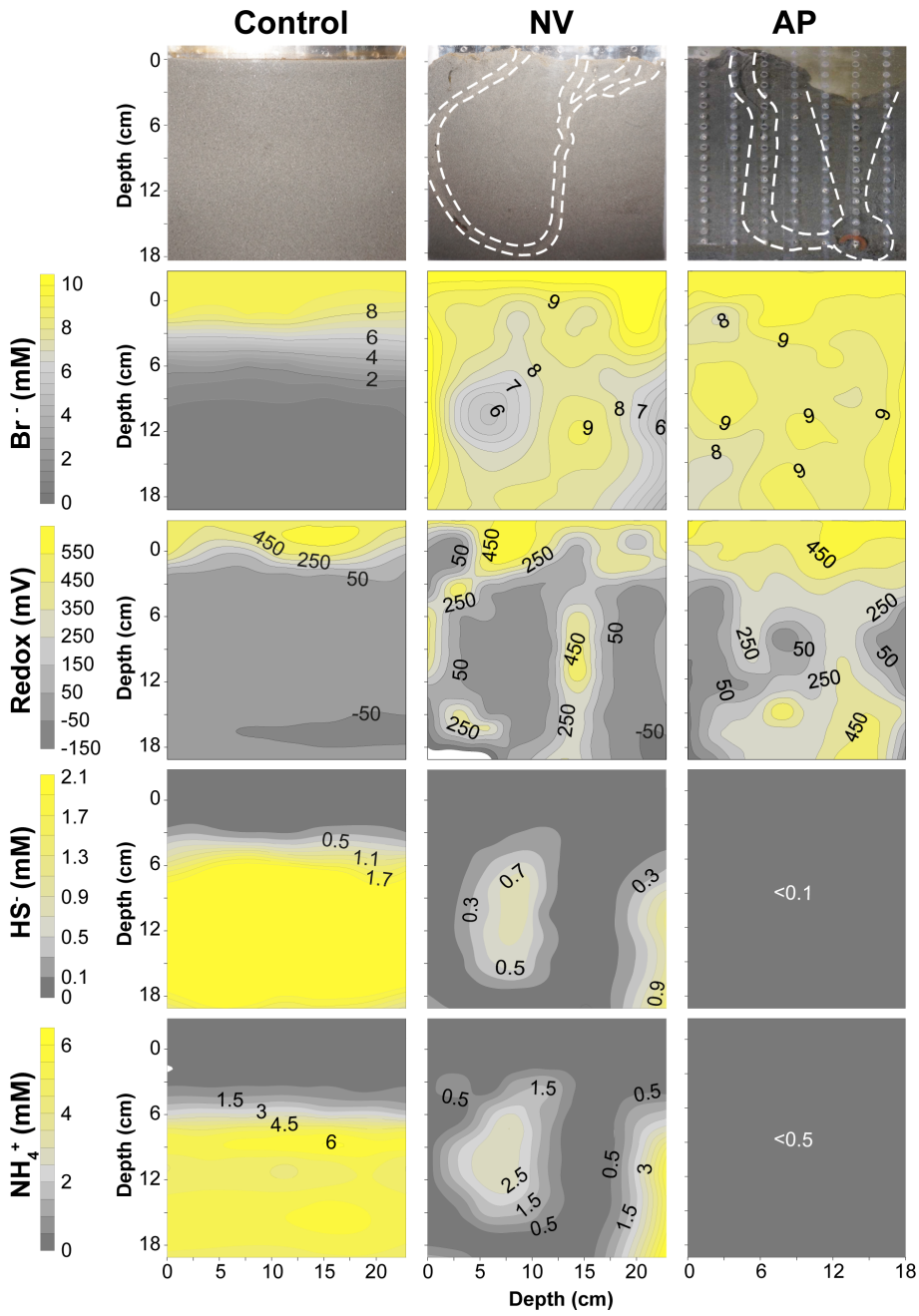

FIGURE 2
Burrow structure, and distributions of the conservative tracer Br^-, redox potential, and metabolic end products (HS^-, NH_4^+) within narrow aquaria after 35 days (T35). [top panel: variations in sediment color are due to differences in light conditions and camera exposure time].

luminophores were detected in deeper layers at T35 (maximum depth: NV = 5 cm, AP = 15 cm). The particle mixing index (M_i) indicates particle mixing throughout the AP feeding funnel and in the upper 5 cm around NV burrows.

*Ochrophyta rbc*L copy numbers, which are dominated by benthic diatoms in False Bay, were used as a proxy for reactive OC (Deng et al., 2022). *Ochrophyta* gene copies were 10^5-10^6 g^{-1} in most samples (Figure 4). Compared to controls, copy numbers were not different in NV treatments (all $p>0.05$, Welch's t test, which will be used here and in the following sections), but were 30-60% (T21) and 40-70% (T35) lower in AP treatments (all $p<0.05$). Within AP treatments, gene copies were lower in feeding funnels (~40% lower) and feces (~90% lower) than in ambient sediments.

A further proxy for reactive OC, chlorophyll *a* (chl *a*), varied mostly from 1-3 μg g^{-1} across treatments and timepoints. Compared to controls, chl *a* was comparable in NV treatments and AP ambient samples (all $p>0.05$), but lower in AP feeding funnels (26-31%; $p<0.05$).

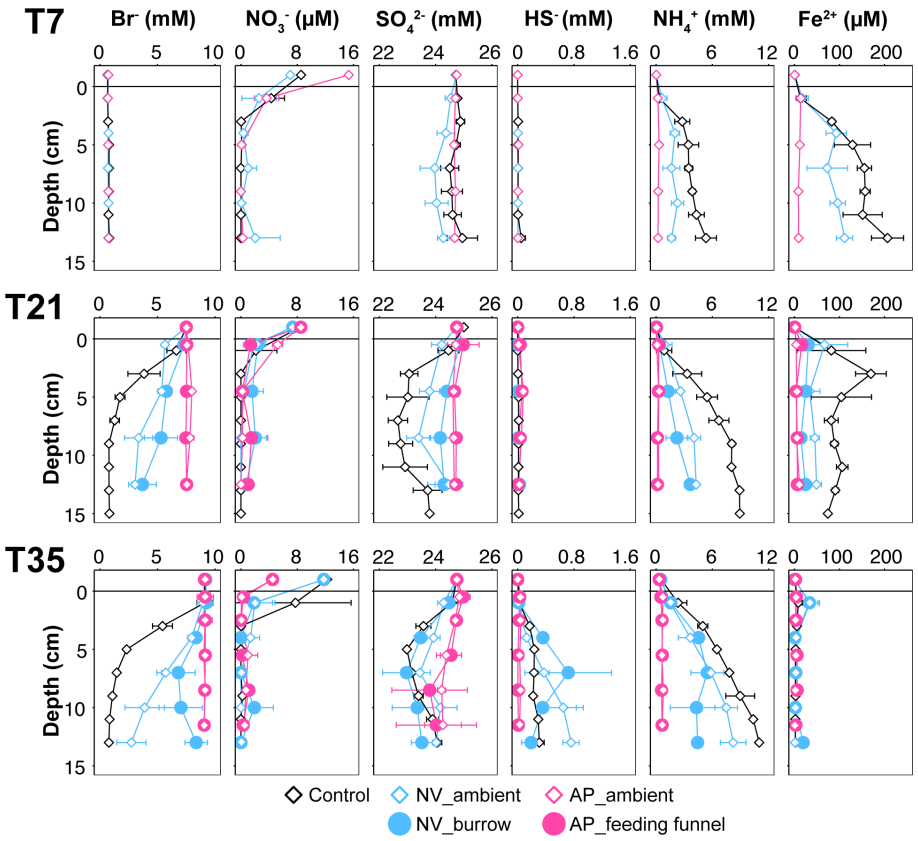

FIGURE 3
Porewater geochemical gradients of wide aquaria through time (T7 = 7 days, T21 = 21 days, T35 = 35 days). Error bars denote the data range of replicate measurements. [Bromide (Br^-) addition was initiated after 15 days.].

3.4 Microbiological impacts of worm bioturbation in wide aquaria

3.4.1 Abundances of 16S rRNA genes and 16S rRNA

Bacterial and archaeal 16S rRNA gene (DNA) copy numbers were lower in NV and AP treatments relative to controls (Figure 5, upper row; $p<0.05$). Bacterial and archaeal 16S rRNA (RNA) copy numbers had similar or slightly lower values in NV treatments compared to controls, and were consistently lower in AP treatments compared to controls, with the lowest values in feeding funnels (Bacteria: -45 ± 18%; Archaea: -69 ± 18%; both $p<0.05$) and fecal samples (Bacteria: -83 ± 13%; Archaea: -98 ± 10%; Figure 5, lower row). Due to stronger decreases in Archaea than in Bacteria, DNA- and RNA-based Bacteria : Archaea Ratios (BARs) were higher in NV (+10 to +70%) and AP treatments (+100 to +540%; $p<0.05$), with the highest ratios measured in feeding funnels.

3.4.2 Bacterial community composition

ZOTU-level analyses of 16S rRNA gene sequences suggest a clear impact of AP but not NV on bacterial community composition (Figures 6A-C). Relative to controls, Shannon indices based on ZOTUs were lower in AP treatments ($p<0.05$) but not in NV treatments (Figure 6A). Moreover, ZOTU-level PCoAs indicate distinct community structures in AP treatments (PERMANOVA; $R^2 = 0.24$, $p<0.05$) but not NV treatments relative to controls ($p>0.05$), and significantly different community structures between AP and NV treatments ($p<0.05$; Figure 6B). The same general trends that were observed for DNA ZOTUs were also observed for RNA ZOTUs (Figure S4).

DNA-based phylogenetic analyses further suggest that AP, but not NV, strongly altered bacterial community composition at the family-level (Figure 6C). Dominant families across treatments include *Planctomycetaceae* (*Planctomycetes*), *Desulfobacteraceae*, *Desulfobulbaceae* (both *Deltaproteobacteria*), *Rhodobiaceae* (*Alphaproteobacteria*), *Flavobacteriaceae* (*Bacteroidetes*), OM1 clade and *Acidimicrobiaceae* (both *Actinobacteria*). Compared to Control and NV treatments, however, AP treatments had lower fractions of *Flavobacteriaceae* and *Rhodobacteracea* and higher fractions of *Planctomycetaceae*, *Desulfobulbaceae*, *Desulfobacteraceae*, OM1 clade, and *Acidimicrobiaceae*, especially in surface and bottom layers, and feces. Within NV treatments, distinct communities, dominated by *Oceanospirillaceae* (*Gammaproteobacteria*), *Campylobacteraceae* (*Epsilonproteobacteria*), and *Rhodobiaceae* (*Alphaproteobacteria*), were only detected in mucus samples.

The dominant families in DNA libraries were also found in RNA libraries, indicating that they were alive and most likely metabolically active (Figure S4). Yet, there were notable differences, e.g. bacterial lineages affiliated with Candidatus *Thiobios*, *Thiotrichacea*, *Chromatiaceae* (all *Gammaproteobacteria*) and with Ca.

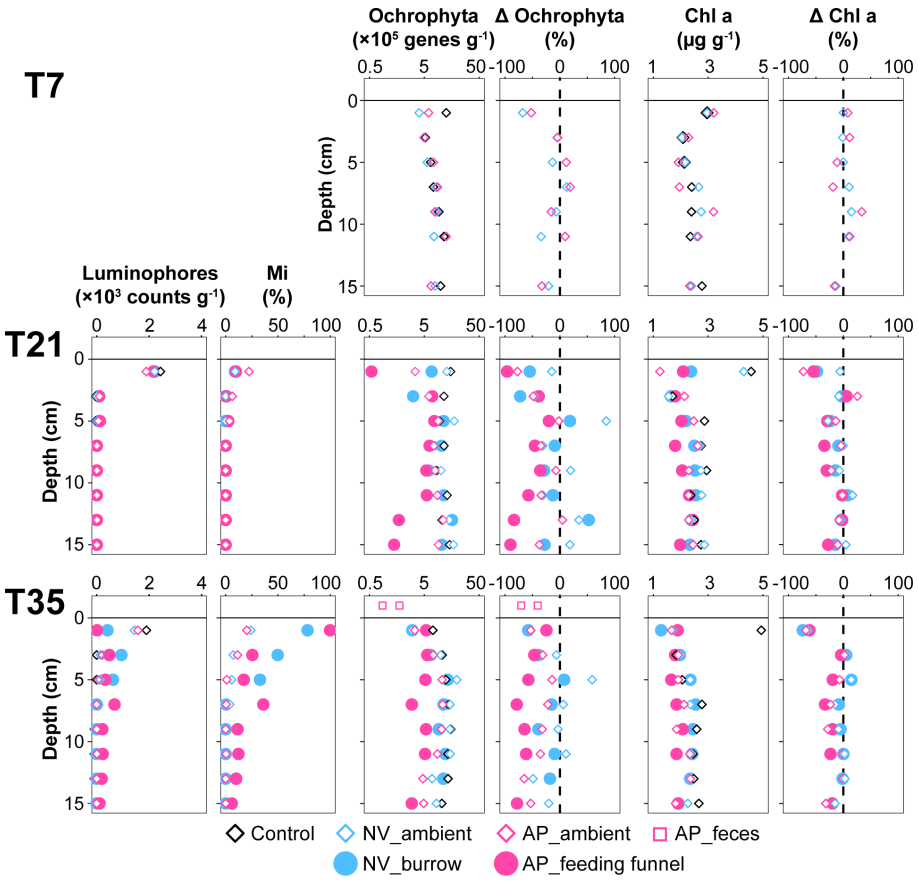

FIGURE 4
Depth profiles of luminophores, particle mixing index (M_i), gene copy numbers of *Ochrophyta rbc*L and chlorophyll *a* (chl *a*) content in wide aquaria. The changes (Δ) of *Ochrophyta*, and chl *a* were calculated from differences between faunal treatments and controls. Luminophores were added 15 days after the initiation of the experiments.

Alysiosphaera (*Alphaproteobacteria*) accounted for higher percentages of RNA sequences, whereas fractions of *Planctomycetaceae*, *Desulfobulbaceae*, *Sandaracinaceae*, *Flavobacteriacea*, OM1 clade and *Acidimicrobiaceae* were lower among RNA sequences. Moreover, while compositions were similar between controls and NV treatments, AP treatments had higher fractions of *Planctomycetaceae* and Ca. *Alysiosphaera* and lower fractions of *Anaerolineacea*, *Rhodobacteracea*, and *Flavobacteraceae*.

3.4.3 Archaeal community composition

ZOTU analyses of 16S rRNA gene sequences indicate a slightly lower archaeal diversity in AP and NV treatments compared to controls (Figure 6D). Nonetheless, archaeal community structure was highly similar across treatments, only differing strongly in surface sediments of AP treatments (Figure 6E). Similar trends were observed at the RNA-level based on 16S rRNA ZOTUs (Figure S4).

Both DNA and RNA sequence analyses revealed the dominance of *Nitrosopumilales* (*Nitrososphaerota*) in AP surface sediments (0-4 cm) and feces (Figures 6F, S4). By contrast *Woesearchaeota*, *Bathyarchaeota* (mainly Group C3 (MCG-15), MCG-8, and MCG-28), and *Euryarchaeota* (mainly Marine Benthic Group D of *Thermoplasmata*) dominated controls, NV sediment and mucus samples, and below 4 cm in AP treatments. As in Bacteria, the same taxa dominated archaeal DNA and RNA sequences, but taxa contributions differed in some cases. Most notably, the beta subgroup of *Lokiarchaeota* and *Thermoplasmata* constituted higher fractions of RNA sequences, while *Woesearchaeota* accounted for higher percentages of DNA sequences.

3.4.4 Impact of bioturbation on microbial activity

Depth-integrated net consumption rates (Figure 7A) show that – compared to controls - O_2 consumption rates were ~2 and ~4-10 times higher, and NO_3^- consumption rates ~4 and ~8-20 times higher in NV and AP treatments, respectively. By contrast, SO_4^{2-} consumption rates were more similar across treatments, being slightly elevated in NV_ambient sediment and lowest in AP feeding funnels.

Similar trends are evident in microbial cell-specific consumption rates (Figure 7B). Compared to controls, cell-specific rates of O_2 consumption were on average ~3 and ~15-40 times higher in NV and AP treatments, respectively. Similarly, cell-specific rates of NO_3^- consumption were ~10-20 and ~25-75 times higher in NV and AP treatments, respectively, compared to controls. By contrast, cell-specific rates of SO_4^{2-} consumption were relatively uniform across treatments (0.5-1 fmol cell^{-1} d^{-1}).

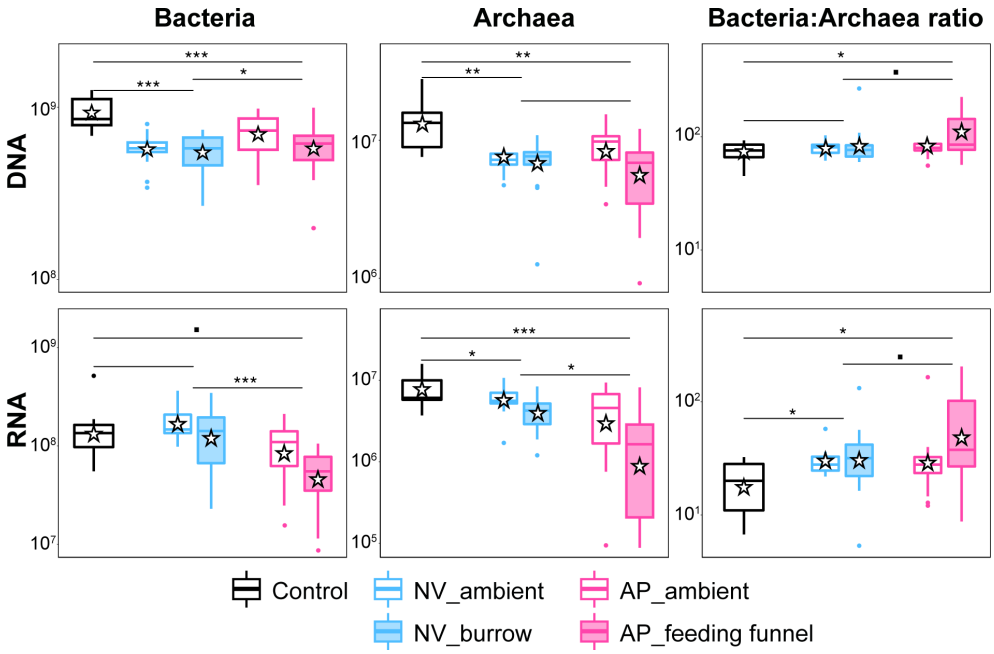

FIGURE 5
Copy numbers of bacterial and archaeal 16S rRNA genes (DNA) and 16S rRNA (RNA), and their ratios (Bacteria:Archaea ratio) across different treatments of wide aquarium incubations at T35. The NV mucus sample and both AP fecal samples are shown in the same columns as NV burrow and AP feeding funnel samples. In boxplots, the boxes show 25% and 75% of the values; horizontal lines and star-shape symbols within the boxes show the medium and mean values; respectively; the whiskers show the entire range of data excluding the statistical outliers. Welch's t tests with Bonferroni-Holm correction were used to compare the group mean of microbial abundance across Control, NV, and AP treatments [***p<0.001, **p<0.01, *p<0.05, ▪p<0.1].

3.5 Overview of how different bioturbation activities affect microbial community structure and metabolic rates

Pearson correlations suggest an overall stronger impact of reworking than ventilation on microbial communities in this experiment (Figure 8). Sediment reworking rates (mixing index) are negatively correlated with bacterial and archaeal abundance and diversity, and show significant correlations with bacterial (DNA and RNA) and archaeal community structure (only DNA). Most bacterial and all archaeal community parameters are also positively correlated with the reactive OC proxy *Ochrophyta rbc*L gene copies, but not chl *a*. By contrast, a clear (negative) correlation of ventilation rates (bioirrigation coefficient, Br^-) was only observed with archaeal abundances and activity. Lastly, cell-specific rates of O_2 and NO_3^- consumption were (mostly) positively correlated with ventilation rates based on the bioirrigation coefficient.

4 Discussion

Burrowing macrofauna are nearly ubiquitous across the seafloor, where they have profound impacts on the transport, transformation, and storage of sedimentary OC (Aller, 1982; Kristensen, 2001; Snelgrove et al., 2018; Bianchi et al., 2021). Recent studies on intertidal, nearshore, and continental margin sediments have indicated a strong impact of benthic macrofauna on microbial communities, and proposed mechanisms by which these macrofauna are altering microbial community structure (Chen et al., 2017; Deng et al., 2020; Deng et al., 2022). Here we experimentally test the predictions of these field studies using microcosm experiments with two functionally distinct species of the globally widespread lugworm and clam worm clades, *Abarenicola pacifica* (AP) and *Nereis vexillosa* (NV). In the following, we first discuss how rates of ventilation and reworking by both species affect sediment geochemistry and microbial activity. Thereafter, we analyze the mechanisms by which ventilation and reworking are affecting assemblages of marine sediment Bacteria and Archaea.

4.1 Worm ventilation rates and their impacts on microbial processes

AP strongly enhances the transport and turnover of porewater solutes by flushing (bioirrigating) the entire sediment layer that it inhabits. The modelled bioirrigation coefficient of 0.3-0.8 d^{-1} corresponds to a turnover time of 1.3-3.3 days for the entire sediment porewater in AP aquaria, and equals pumping rates of 35-93 ml $individual^{-1}$ h^{-1}. These rates are in the range of reported pumping rates for AP and its close relative *Arenicola marina* based on laboratory studies (15-100 ml h^{-1}; Riisgård, et al., 1996; Kristensen, 2001; Timmermann et al., 2006; Volkenborn et al., 2010; Dornhoffer et al., 2015) and field studies (Deng et al., 2022). Compared to controls, AP increases the consumption of oxygen 4- to 10-fold and nitrate 8- to 20-fold. This is in the same range or

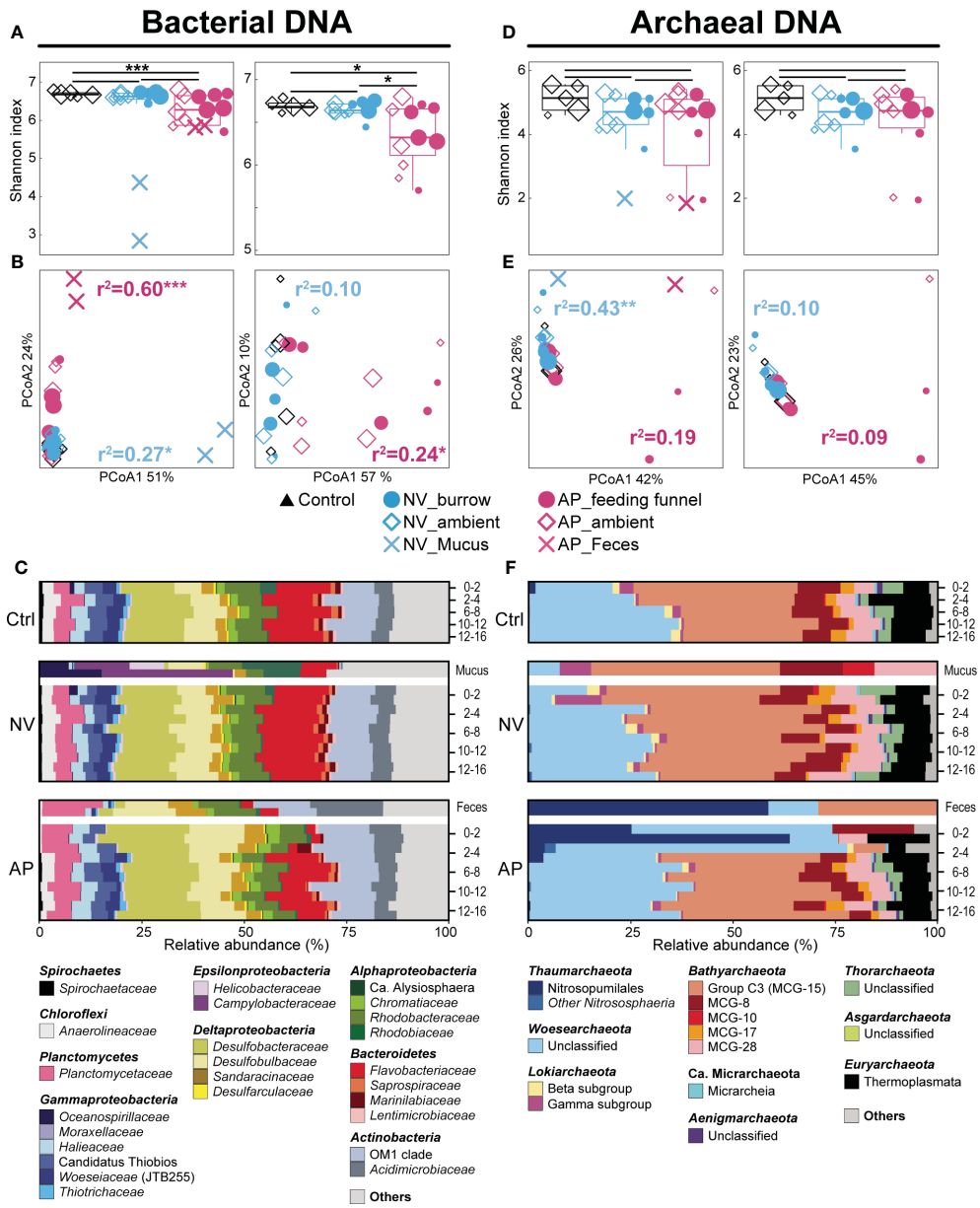

FIGURE 6
Impact of worm bioturbation on 16S rRNA gene based microbial community composition in wide aquaria at T35. Within **(A, B, D, E)** the left and right panels are based on analyses that include and exclude faunal mucus and feces samples, respectively. The symbol size is proportional to sediment depth. **(A, D)** Shannon diversity based on ZOTUs. Welch's t tests with Bonferroni-Holm correction are used to compare the group mean of Shannon diversity across different treatments [***p<0.001, **p<0.01, *p<0.05, ■p<0.1]. **(B, E)** Principal Coordinates Analysis (PCoA) on microbial community composition based on ZOTUs. r^2-values indicate dissimilarity of worm treatments relative to controls based on PERmutational Multivariate ANalysis Of VAriance (PERMANOVA). [***p<0.001, **p<0.01, *p<0.05, ■p<0.1]. **(C, F)** Relative abundance of dominant microbial taxa based on 16S rRNA gene sequences. Depth intervals in cm are indicated on y-axes. For fauna treatments, each interval includes two samples (top bar: burrow/feeding funnel; bottom bar: ambient).

higher than in other strong ventilators such as *Arenicola marina* and thalassinidean shrimps based on laboratory studies (Banta et al., 1999; Howe et al., 2004). By contrast, net consumption rates of sulfate are less affected and even 50% lower in the AP feeding funnel compared to controls, possibly due to inhibition of microbial sulfate reduction by the high input of energetically superior electron acceptors, such as O_2 and NO_3^- (Figure 7). While AP likely increases the ammonium turnover, it also lowers NH_4^+ concentrations, presumably due to both ventilative flushing out of the sediment and increased microbial consumption. If we conservatively assume that OM degradation rates, and hence NH_4^+ production rates, are the same in AP treatments as in controls, then – based on a bioirrigation rate of 0.3 d^{-1} – ~30-70% of the produced NH_4^+ is removed by flushing. This would leave the remainder for microbial consumption, e.g., by nitrification (Figure S5).

By comparison, NV has a weaker impact on sediment biogeochemistry, that mainly results from burrow ventilation. Herein most of the water that is introduced by ventilation flows

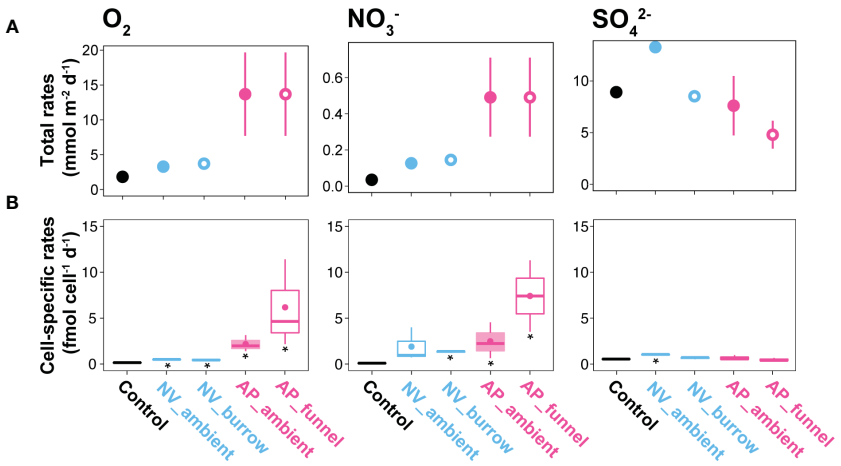

FIGURE 7
Net consumption rates of O_2, NO_3^-, and SO_4^{2-} across treatments in wide aquaria. **(A)** Depth-integrated total consumption rates. In AP treatments, error bars indicate the modeled range of consumption rates, which were derived from the upper and lower limits of bioirrigation intensity of A *pacifica*, and the circles denote the median values. **(B)** Cell-specific reaction rates. The error ranges reflect the variations of estimated cell numbers of specific functional groups across different samples in the same treatment. For details, see Materials and Methods.

out of the burrow again. As a result, NV mainly promotes diffusive rather than advective exchanges across the burrow wall, which explains the localized impact of ventilation on sediments surrounding burrows. Geometric measurements, which show an average burrow length of ~55 cm and burrow diameter of 2 cm, suggest that burrows of three NV individuals increase the sediment-water interface by ~140% in our wide aquaria. Molecular diffusion of Br^- across this increased sediment-water interface explains ~60% of the increase in Br^- concentrations in NV treatments, with the remainder being likely due to advective irrigation. As a result, the stimulation of oxygen and nitrate removal in sediments with NV is much lower compared to more strongly bioirrigated AP-inhabited sediments (Figure 7).

4.2 Deposit-feeding greatly accelerates the cycling of reactive OM in sediment

Our results indicate that *Nereis vexillosa* performs minimal sediment reworking (Figure 4). Most of this reworking can be explained with burrow maintenance rather than deposit-feeding, as repeated burrow repair was observed at burrow openings and luminophores were only transported to deeper sediment layers (≤5 cm) near burrow openings (Figure 4). By contrast, *Abarenicola pacifica* not only reworks sediments for burrow maintenance and construction, but additionally – and much more so – by being a very active subsurface deposit feeder. Based on field research, it has been proposed that this subsurface deposit-feeding by AP accelerates the cycling of reactive OM, mainly through selective feeding on fine-grained sediment that is rich in microalgal OM (Hylleberg, 1975; Deng et al., 2022). Our experiments confirm this observation. We measure significant decreases in *Ochrophyta rbc*L gene copy numbers in AP treatments (by 30-90%), with the strongest decreases in feces and feeding funnels, where the impact of feeding is maximal (Figure 4). While numerical models have suggested that bioirrigation by lugworms has a greater impact on sedimentary OC degradation than reworking by shear particle mixing (Kristensen, 2001), our results indicate that – assuming that most of the OC cycling is driven by the production and consumption of microphytobenthic biomass – AP reworking by deposit-feeding has an even greater impact on OC cycling than bioirrigation in the sediments studied.

Notably, the abundance of *Ochrophyta* genes decreases much more than chl *a* content in AP treatments. This indicates that *Ochrophyta* gene copy numbers are a more sensitive proxy to study the impact of deposit feeding on labile, microphytobenthic OM in the sediments studied. A potential reason is that diatom DNA is more labile, and thus more rapidly remineralized during AP gut passage, than diatom chl *a*. In addition, it is possible that a major fraction of the chl *a* in the sediments studied is present in a low-reactivity detrital form, or as large macroalgal or seagrass detrital particles that are selectively avoided by feeding AP (Lopez and Levinton, 1987).

4.3 Deposit-feeding as a key driver of bacterial abundance and community structure

Our microcosm experiments with AP provide the first experimental support that macrofaunal reworking by deposit-feeding controls bacterial abundance and community structure throughout the entire bioturbated layer (Chen et al., 2017; Deng et al., 2020; Deng et al., 2022). Correlation analyses indicate that reworking by sediment mixing (mixing index, luminophores) and deposit feeding (*rbc*L *Ochrophyta* gene copy) impacts bacterial abundance and community structure much more than ventilation (bioirrigation coefficient, Br^- concentration) (Figure 8). The only minor impact of ventilation, despite its strong impact on electron acceptor distributions and redox conditions (Figures 2, 3, S2)

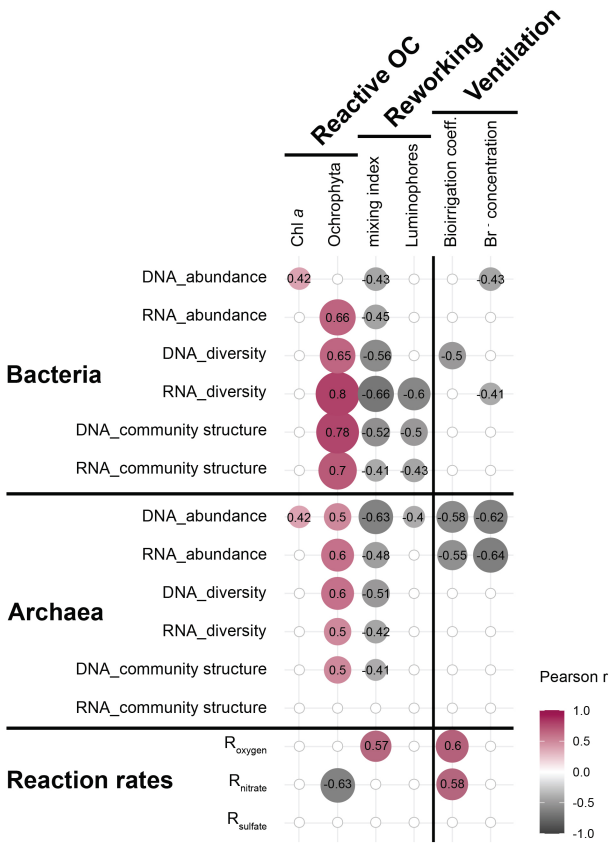

FIGURE 8
Pearson correlations of bacterial and archaeal abundance, Shannon diversity, and community structure with proxies for macrofaunal reworking and ventilation (includes all samples and treatments from T35 (Figure 6); n=27). Variations in microbial community structure are represented by the first PCoA axes (Figures 6B, E), which capture the maximal variances of wunifrac-distance matrices calculated from ZOTU tables and phylogenetic distances. In addition, Pearson correlations between cell-specific turnover rates of O_2, NO_3^-, and SO_4^{2-} and proxies for macrofaunal reworking and ventilation are included ('Reaction rates'). Only significant correlations ($p<0.05$) are shown.

supports the inference from our field study on AP that bacterial populations in intertidal sediments in False Bay are highly redox-resilient (Deng et al., 2022). This redox-resilience could be due to the ability of many bacteria in marine surface sands to switch between aerobic and anaerobic modes of energy generation (Kessler et al., 2019).

We propose that the negative impact of AP reworking on bacterial abundance is directly related to selective feeding by AP on microalgal detritus, and support this proposition based on three lines of reasoning. First, bacterial 16S rRNA copy numbers are highly correlated with *rbc*L *Ochrophyta* gene copy numbers, suggesting that diatom detritus is populated by large populations of (organoheterotrophic) bacteria. Second, copy numbers of 16S rRNA decrease more strongly in response to AP feeding than those of 16S rRNA genes. This could indicate that active, rapidly growing bacteria that are associated with labile microalgal detritus are either ingested at a higher rate by AP or more likely to undergo cell lysis and digestion during AP gut passage. Third, we observe major variations in bacterial community structure in relation to *rbc*L *Ochrophyta* copy numbers and major phylogenetic shifts in AP treatments (Figure 8). Those bacterial groups that are most negatively impacted by AP are putative algae degraders. For instance, the algal polysaccharide degrader *Flavobacteriia* (mainly *Flavobacteriaceae*, Hoffmann et al., 2017) experienced the strongest decreases in relative and absolute abundances. Likewise, the abundances of most ZOTUs of *Bacteroidetes* (*Saprospiraceae*, *Marinilabiaceae*) and *Alphaprotebacteria* (*Rhodobacteraceae*), which include many algal biomass degraders or algal symbionts (McIlroy and Nielsen, 2014; Pujalte et al., 2014), decreased strongly (Figure S6).

4.4 Bioirrigation as the main driver of archaeal abundance and community structure

While sediment reworking rates also correlate strongly with archaeal abundance and community structure, the correlations are slightly weaker compared to those with Bacteria. Yet, unlike Bacteria, DNA- and RNA-based abundances of Archaea show significant negative correlations with bioirrigation coefficients and Br^- concentrations, suggesting a strong negative impact of bioirrigation on archaeal abundances (Figure 8). This observation matches past field studies which proposed a strong impact of

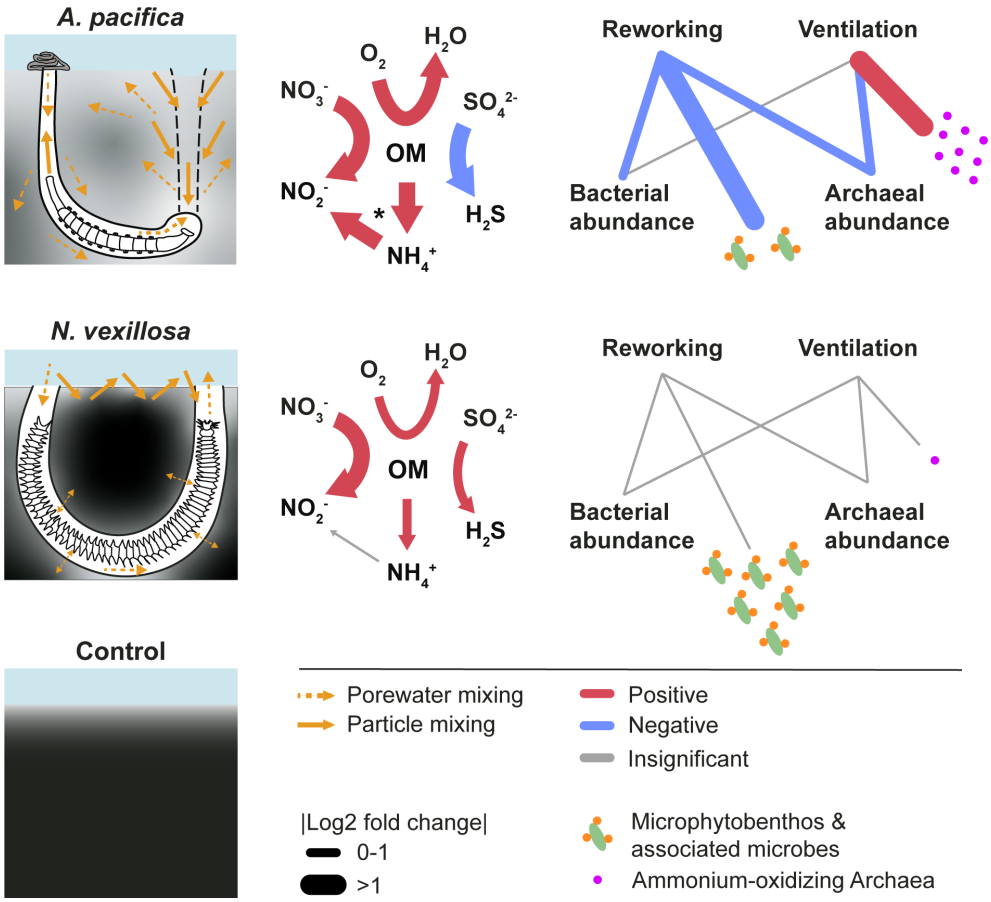

FIGURE 9
Conceptual diagram summarizing the distinct impacts of *A. pacifica* and *N. vexillos* on sediment biogeochemical processes and microbial communities. Leftmost panels: Porewater ventilation and sediment reworking activities of the two worm species (based on Figures 1-3, S2). *A. pacifica* activity profoundly impacts porewater and particle mixing throughout, whereas *N. vexillosa* impacts porewater and particle mixing mainly in surface sediments and around burrows. As a result, *A. pacifica* elevates the redox potential in sediment above its burrow (light gray background color), while sediments away from *N. vexillosa* burrows and in controls are highly reducing (black color). Middle panels: Worm impacts on major biogeochemical reactions (mainly based on Figure 7). The color and thickness of arrows indicate the direction (positive or negative) and extent of macrofaunal impact and are based on log2-fold changes in reaction rates relative to controls [* the enhanced gross NH_4^+ production and oxidation in *A. pacifica* treatments is inferred from the observed decrease in reactive organic matter, the dominance of nitrifying Archaea in surface sediment, and the modelled low net NH_4^+ production rates.] Rightmost panels: Impact of *A. pacifica* and *N. vexillosa* on benthic microbial communities (based on Figures 4-6). The color and thickness of lines indicate the impact of macrofaunal reworking (mainly deposit feeding) and ventilation on the abundances of Bacteria, Archaea, microalgae-associated microbes (represented by *Flavobacteriia*), and nitrifying Archaea (*Nitrosopumilus*).

macrofaunal ventilation on archaeal community structure in continental shelf sediment (Deng et al., 2020). One possible explanation for this trend is lower tolerance of Archaea to redox fluctuations compared to Bacteria. This was previously proposed based on elevated Bacteria to Archaea ratios (BARs) in bioturbated coastal and continental margin sediments (Chen et al., 2017; Deng et al., 2020), and is now supported by controlled laboratory experiments in this study.

Despite the overall negative impact of ventilation on archaeal abundance, a single ZOTU with >99% 16S rRNA gene sequence similarity to the aerobic ammonium oxidizing *Nitrosopumilus oxyclinae* (order *Nitrosopumilales*) seems to greatly benefit from macrofaunal ventilation activity, though only in AP treatments. This ZOTU increases 30- to 40-fold in relative abundance and 10-15 fold in absolute abundance in surface sediments (0-4 cm) of AP treatments compared to controls (Figures 6F, S6). We explain the high abundances of this ZOTU, which even dominates archaeal communities in surface sediments of AP treatments, with high O_2 availability. Even though O_2 was not measurable below the top few mm, lugworms are known to effectively pump dissolved oxygen through surface sediments both during 'forward pumping', where overlying water enters *via* the tail shaft and is pumped through the feeding funnel, as well as during 'backward pumping', where this water flow is reversed (Volkenborn et al., 2010). The observed increase of *Nitrosopumilus* matches the highly elevated abundance of this group in ventilated coastal and continental shelf sediments

(Chen et al., 2017; Deng et al., 2020) and is aligned with the notion that bioirrigation is a major driver of ammonia-oxidizing archaeal distributions and nitrification in marine sediments.

4.5 Impact of bioturbation on cell-specific reaction rates

Our data further suggest that bioturbation affects sediment biogeochemical cycles not only by regulating microbial metabolism and community composition, but also by strongly affecting cell-specific reaction rates (Figure 7). While the stimulation of microbial processes, such as oxic respiration and denitification, by bioturbation was previously observed (Banta et al., 1999; Howe et al., 2004), it has remained unclear whether this stimulation is due to increased microbial abundance or cell-specific reaction rates (Bertics and Ziebis, 2009; Laverock et al., 2011; Laverock et al., 2013; Poulsen et al., 2014). Our data indicate clear increases in cell-specific rates of O_2 and NO_3^- consumption in both NV and AP treatments (Figure 7). These increased cell-specific rates override the significantly lower microbial abundances in bioturbated sediments, as evidenced by higher total O_2 and NO_3^- consumption rates in NV and AP treatments compared to macrofauna-free controls.

5 Conclusions

By integrating analyses of bioturbation activity, sediment geochemistry, and biogeochemical process rates with analyses of microbial community dynamics we show that two functionally distinct polychaete groups differ greatly in their impacts on sedimentary ecosystems (Figure 9). The lugworm *A. pacifica* is a strong bioturbator that drives the rapid turnover of reactive OM and metabolic end products, and through its deposit-feeding activity selects for a small, yet highly active, microbial community. By contrast, the clamworm *N. vexillosa*, which foremost utilizes subsurface sediments for protective shelter, neither performs deposit-feeding nor strong bioirrigation, and consequently has a vastly lower impact on sediment biogeochemical processes and microbial communities. The stark differences in impacts between these two species highlight the importance of using experiments to verify links between macrofauna, macrofaunal activity, and microbial populations inferred from field data, and demonstrates the necessity to incorporate macrofaunal distribution maps into biogeochemical models at regional to global scales (Snelgrove et al., 2018; Bianchi et al., 2021).

Data availability statement

The datasets presented in this study can be found on the webpage of the National Center for Biotechnology Information (https://www.ncbi.nlm.nih.gov/; PRJNA773619) and in the Supplementary Material.

Author contributions

LD and ML designed the study with input from AF and DB; LD, AF, and DB conducted the sampling and laboratory experiments; LD, AF, DB, DM, CM, and ML performed measurements and/or data analysis; LD, CM, and ML wrote the manuscript with input from all co-authors. All authors agree to be accountable for the content of the work. All authors approved the submitted version.

Funding

This study was funded by the Swiss National Science Foundation Project 205321_163371 (ML). CM was funded by the National Science Foundation Long-Term Ecological Research program NSF OCE-1832178 (CM). Open access funding provided by ETH Zurich.

Acknowledgments

We thank Bernadette Holthuis, Jeannie Meredith, Megan Dethier, Michelle Herko, Stacy Markman (Friday Harbor Laboratories, University of Washington) for providing administrative and scientific supports during the sampling campaign in the False Bay Biological Preserve; Iso Christl and Ruben Kretzschmar (Soil Chemistry group, ETH Zurich) for sharing instrument and assistance with dissolved metal analysis. Amplicon sequencing data produced and analyzed in this paper were generated in collaboration with the Genetic Diversity Centre (GDC), ETH Zurich. This is Nereis Park contribution #43.

Conflict of interest

The authors declare that the research was conducted in the absence of any commercial or financial relationships that could be construed as a potential conflict of interest.

Publisher's note

Supplementary material

The Supplementary Material for this article can be found online at: https://www.frontiersin.org/articles/10.3389/fmars.2023.1119331/full#supplementary-material

References

Aller, R. C. (1982). "The effects of macrobenthos on chemical properties of marine sediment and overlying water," in *Animal-sediment relations* (Boston, MA: Springer), 53–102. doi: 10.1007/978-1-4757-1317-6_2

Aller, R. C. (1990). Bioturbation and manganese cycling in hemipelagic sediments. *Philos. Trans. R. Soc. a-Mathematical Phys. Eng. Sci.* 331 (1616), 51–68. doi: 10.1098/rsta.1990.0056

Banta, G. T., Holmer, M., Jensen, M. H., and Kristensen, E. (1999). Effects of two polychaete worms, nereis diversicolor and arenicola marina, on aerobic and anaerobic decomposition in a sandy marine sediment. *Aquat. Microbial Ecol.* 19 (2), 189–204. doi: 10.3354/ame019189

Bertics, V. J., and Ziebis, W. (2009). Biodiversity of benthic microbial communities in bioturbated coastal sediments is controlled by geochemical microniches. *ISME J.* 3 (11), 1269–1285. doi: 10.1038/ismej.2009.62

Bianchi, T. S., Aller, R. C., Atwood, T. B., Brown, C. J., Buatois, L. A., Levin, L. A., et al. (2021). What global biogeochemical consequences will marine animal–sediment interactions have during climate change? *Elem Sci. Anth.* 9 (1), 180. doi: 10.1525/elementa.2020.00180

Cahoon, L. B. (2002). The role of benthic microalgae in neritic ecosystems. *Oceanogr. Marine Biol.* 37, 47–86.

Chen, X., Andersen, T. J., Morono, Y., Inagaki, F., Jorgensen, B. B., and Lever, M. A. (2017). Bioturbation as a key driver behind the dominance of bacteria over archaea in near-surface sediment. *Sci. Rep.* 7 (1), 2400. doi: 10.1038/s41598-017-02295-x

Cline, J. D. (1969). Spectrophotometric determination of hydrogen sulfide in natural waters 1. *Limnology Oceanography* 14 (3), 454–458. doi: 10.4319/lo.1969.14.3.0454

Cuny, P., Miralles, G., Cornet-Barthaux, C., Acquaviva, M., Stora, G., Grossi, V., et al. (2007). Influence of bioturbation by the polychaete nereis diversicolor on the structure of bacterial communities in oil contaminated coastal sediments. *Mar. Poll Bull.* 54, 452–549. doi: 10.1016/j.marpolbul.2006.12.008

Dale, H., Taylor, J. D., Solan, M., Lam, P., and Cunliffe, M. (2019). Polychaete mucopolysaccharide alters sediment microbial diversity and stimulates ammonia-oxidising functional groups. *FEMS Microbiol. Ecol.* 95 (2), fiy234. doi: 10.1093/femsec/fiy234

de Beer, D., Wenzhöfer, F., Ferdelman, T. G., Boehme, S. E., Huettel, M., van Beusekom, J. E., et al. (2005). Transport and mineralization rates in north Sea sandy intertidal sediments, sylt-rømø basin, wadden Sea. *Limnology Oceanography* 50 (1), 113–127. doi: 10.4319/lo.2005.50.1.0113

Deng, L., Bölsterli, D., Kristensen, E., Meile, C., Su, C., Bernasconie, S. M., et al. (2020). Macrofaunal control of microbial community structure in continental margin sediments. *Proc. Natl. Acad. Sci.* 117 (27), 15911–15922. doi: 10.1073/pnas.1917494117

Deng, L., Fiskal, A., Han, X., Dubois, N., Bernasconie, S. M., and Lever, M. A. (2019). Improving the accuracy of flow cytometric quantification of microbial populations in sediments: importance of cell staining procedures. *Front. Microbiology* 10, 720. doi: 10.3389/fmicb.2019.00720

Deng, L., Meile, C., Fiskal, A., Bölsterli, D., Han, X., Gajendra, N., et al. (2022). Deposit-feeding worms control subsurface ecosystem functioning in intertidal sediment with strong physical forcing. *PNAS Nexus* 1 (4), pgac146. doi: 10.1093/pnasnexus/pgac146

Dornhoffer, T. M., Waldbusser, G. G., and Meile, C. (2015). Modeling lugworm irrigation behavior effects on sediment nitrogen cycling. *Mar. Ecol. Prog. Series 534*, 121–134. doi: 10.3354/meps11381

Fenchel, T. (1970). Studies on the decomposition of organic detritus derived from the turtle grass thalassia testudinum 1. *Limnology Oceanography* 15 (1), 14–20. doi: 10.4319/lo.1970.15.1.0014

Fiskal, A., Deng, L., Michel, A., Eickenbusch, P., Han, X., Lagostina, L., et al. (2019). Effects of eutrophication on sedimentary organic carbon cycling in five temperate lakes. *Biogeosciences* 16 (19), 3725–3746. doi: 10.5194/bg-16-3725-2019

Gilbert, F., Stora, G., and Bonin, P. (1998). Influence of bioturbation on denitrification activity in Mediterranean coastal sediments: an *in situ* experimental approach. *Mar. Ecol. Prog. Ser.* 163, 99–107. doi: 10.3354/meps163099

Healy, E. A., and Wells, G. P. (1959). "Three new lugworms (Arenicolidae, polychaeta) from the north pacific area," in *Proceedings of the zoological society of London*. (Oxford, UK: Blackwell Publishing Ltd), 133 315–335. doi: 10.1111/j.1469-7998.1959.tb05565.x

Herman, P. M. J., Middelburg, J. J., and Heip, C. H. R. (2001). Benthic community structure and sediment processes on an intertidal flat: results from the ECOFLAT project. *Continental Shelf Res.* 21 (18), 2055–2071. doi: 10.1016/S0278-4343(01)00042-5

Hobson, K. D. (1967). The feeding and ecology of two North Pacific Abarenicola species (Abarenicolidae, Polychaeta). *Biol. Bull.* 133, 343–354. doi: 10.2307/1539830

Hoffmann, K., Hassenruck, C., Salman-Carvalho, V., Holtappels, M., and Bienhold, C. (2017). Response of bacterial communities to different detritus compositions in Arctic deep-Sea sediments. *Front. Microbiol. 8* 266. doi: 10.3389/fmicb.2017.00266

Howe, R. L., Rees, A. P., and Widdicombe, S. (2004). The impact of two species of bioturbating shrimp (Callianassa subterranea and upogebia deltaura) on sediment denitrification. *J. Mar. Biol. Assoc. United Kingdom* 84 (3), 629–632. doi: 10.1017/S002531540400966Xh

Huettel, M., Berg, P., and Kostka, J. E. (2014). Benthic exchange and biogeochemical cycling in permeable sediments. *Ann. Rev. Mar. Sci. 6*, 23–51. doi: 10.1146/annurev-marine-051413-012706

Hylleberg, J. (1975). Selective feeding byAbarenicola pacificawith notes onAbarenicola vagabundaand a concept of gardening in lugworms. *Ophelia* 14 (1-2), 113–137. doi: 10.1080/00785236.1975.10421972

Kessler, A. J., Chen, Y. J., Waite, D. W., Hutchinson, T., Koh, S., Popa, M. E., et al. (2019). Bacterial fermentation and respiration processes are uncoupled in anoxic permeable sediments. *Nat. Microbiol.* 4 (6), 1014–1023. doi: 10.1038/s41564-019-0391-z

Kristensen, E. (2001). Impact of polychaetes (Nereis spp. and arenicola marina) on carbon biogeochemistry in coastal marine sediments. *Geochemical Trans.* 2 (12), 92. doi: 10.1186/1467-4866-2-92

Kristensen, E., Penha-Lopes, G., Delefosse, M., Valdemarsen, T., Quintana, C. O., and Banta, G. T. (2012). What is bioturbation? the need for a precise definition for fauna in aquatic sciences. *Mar. Ecol. Prog. Ser.* 446, 285–302. doi: 10.3354/meps09506

LaRowe, D. E., Arndt, S., Bradley, J. A., Burwicz, E., Dale, A. W., and Amend, J. P. (2020). Organic carbon and microbial activity in marine sediments on a global scale throughout the quaternary. *Geochimica Cosmochimica Acta* 286, 227–247. doi: 10.1016/j.gca.2020.07.017

Laverock, B., Gilbert, J. A., Tait, K., Osborn, A. M., and Widdicombe, S. (2011). Bioturbation: impact on the marine nitrogen cycle. *Biochem. Soc. Trans.* 39 (1), 315–320. doi: 10.1042/BST0390315

Laverock, B., Kitidis, V., Tait, K., Gilbert, J., Osborn, A., and Widdicombe, S. (2013). Bioturbation determines the response of benthic ammonia-oxidizing microorganisms to ocean acidification. *Philos. Trans. R. Soc. B: Biol. Sci.* 368 (1627), 20120441. doi: 10.1098/rstb.2012.0441

Lever, M. A., Torti, A., Eickenbusch, P., Michaud, A. B., Šantl-Temkiv, T., and Jørgensen, B. B. (2015). A modular method for the extraction of DNA and RNA, and the separation of DNA pools from diverse environmental sample types. *Front. Microbiol.* 6. doi: 10.3389/fmicb.2015.00476

Lever, M. A., and Valiela, I. (2005). Response of microphytobenthic biomass to experimental nutrient enrichment and grazer exclusion at different land-derived nitrogen loads. *Mar. Ecol. Prog. Ser.* 294, 117–129. doi: 10.3354/meps294117

Levin, L., Blair, N., DeMaster, D., Plaia, G., Fornes, W., Martin, C., et al. (1997). Rapid subduction of organic matter by maldanid polychaetes on the north Carolina slope. *J. Mar. Res.* 55 (3), 595–611. doi: 10.1357/0022240973224337

Lopez, G. R., and Levinton, J. S. (1987). Ecology of deposit-feeding animals in marine sediments. *Q. Rev. Biol.* 62 (3), 235–260. doi: 10.1086/415511

Lorenzen, C. J. (1967). Determination of chlorophyll and pheo-pigments: spectrophotometeric equations. *Limnology oceanography* 12 (2), 343–346. doi: 10.4319/lo.1967.12.2.0343

Louca, S., Parfrey, L. W., and Doebeli, M. (2016). Decoupling function and taxonomy in the global ocean microbiome. *Science* 353 (6305), 1272–1277. doi: 10.1126/science.aaf4507

Marinelli, R. L., Lovell, C. R., Wakeham, S. G., Ringelberg, D. B., and White, D. C. (2002). Experimental investigation of the control of bacterial community composition in macrofaunal burrows. *Mar. Ecol. Prog. Ser.* 235, 1–13. doi: 10.3354/meps235001

McIlroy, S. J., and Nielsen, P. H. (2014). "The family saprospiraceae," in *The prokaryotes: other major lineages of bacteria and the archaea*, *4 ed*, vol. 11 . Eds. E. Rosenberg, E. F. Delong, S. Lory, E. Stackebrandt and F. Thompson (Berlin, Heidelberg: Springer), 863–889. doi: 10.1007/978-3-642-38954-2_138

McMurdie, P. J., and Holmes, S. (2013). Phyloseq: an r package for reproducible interactive analysis and graphics of microbiome census data. *PLoS One* 8 (4), e61217. doi: 10.1371/journal.pone.0061217

Mermillod-Blondin, F., Rosenberg, R., François-Carcaillet, F., Norling, K., and Mauclaire, L. (2004). Influence of bioturbation by three benthic infaunal species on microbial communities and biogeochemical processes in marine sediment. *Aquat. Microb. Ecol.* 36, 271–284. doi: 10.3354/ame036271

Middelburg, J. J. (2018). Reviews and syntheses: to the bottom of carbon processing at the seafloor. *Biogeosciences* 15 (2), 413–427. doi: 10.5194/bg-15-413-2018

Miranda, K. M., Espey, M. G., and Wink, D. A. (2001). A rapid, simple spectrophotometric method for simultaneous detection of nitrate and nitrite. *Nitric. Oxide* 5 (1), 62–71. doi: 10.1006/niox.2000.0319

Oksanen, J., Simpson, G. L., Blanchet, F. G., Kindt, R., and Legendre, P. (2013). "Package 'vegan," in *Community ecology package, version*. 2, 1–295. Available at: https://cran.r-project.org/web/packages/vegan/vegan.pdf.

Pamatmat, M. M. (1968). Ecology and metabolism of a benthic community on an intertidal sandflat. *Internationale Rev. der gesamten hydrobiologie und Hydrographie* 53 (2), 211–298. doi: 10.1002/iroh.19680530203

Papaspyrou, S., Gregersen, T., Kristensen, E., Christensen, B., and Cox, R. P. (2006). Microbial reaction rates and bacterial communities in sediment surrounding burrows of two nereidid polychaetes (Nereis diversicolor and n. virens). *Mar. Biol.* 148 (3), 541–550. doi: 10.1007/s00227-005-0105-3

Plante, C., and Jumars, P. (1993). Immunofluorescence assay for effects on field abundance of a naturally occurring pseudomonad during passage through the gut of a marine deposit feeder, abarenicola pacifica. *Microbial Ecol.* 26 (3), 247–266. doi: 10.1007/BF00176957

Plante, C. J., Jumars, P. A., and Baross, J. A. (1989). Rapid bacterial growth in the hindgut of a marine deposit feeder. *Microbial Ecol.* 18 (1), 29–44. doi: 10.1007/BF02011694

Plante, C. J., Jumars, P. A., and Baross, J. A. (1990). Digestive associations between marine detritivores and bacteria. *Annu. Rev. Ecol. Systematics* 21, 93–127. doi: 10.1146/annurev.ecolsys

Plante, C. J., and Shriver, A. G. (1998). Differential lysis of sedimentary bacteria by arenicola marina l.: examination of cell wall structure and exopolymeric capsules as correlates. *J. Exp. Mar. Biol. Ecol.* 229 (1), 35–52. doi: 10.1016/S0022-0981(98)00039-2

Poulsen, M., Kofoed, M. V., Larsen, L. H., Schramm, A., and Stief, P. (2014). Chironomus plumosus larvae increase fluxes of denitrification products and diversity of nitrate-reducing bacteria in freshwater sediment. *Systematic Appl. Microbiol.* 37 (1), 51–59. doi: 10.1016/j.syapm.2013.07.006

Pujalte, M. J., Lucena, T., Ruvira, M. A., Arahal, D. R., and Macián, M. C. (2014). "The family rhodobacteraceae," in *The prokaryotes*. Eds. E. Rosenberg, E. F. DeLong, S. Lory, E. Stackebrandt and F. Thompson (Berlin, Heidelberg: Springer). doi: 10.1007/978-3-642-30197-1_377

Quast, C., Pruesse, E., Yilmaz, P., Gerken, J., Schweer, T., Yarza, P., et al. (2012). The SILVA ribosomal RNA gene database project: improved data processing and web-based tools. *Nucleic Acids Res.* 41 (D1), D590–D596. doi: 10.1093/nar/gks1219

Riisgård, H. U., Berntsen, I., and Tarp, B. (1996). The lugworm (Arenicola marina) pump: characteristics, modelling and energy cost. *Mar. Ecol. Prog. Series 138*, 149–156. doi: 10.3354/meps138149

Satoh, H., Nakamura, Y., and Okabe, S. (2007). Influences of infaunal burrows on the community structure and activity of ammonia-oxidizing bacteria in intertidal sediments. *Appl. Environ. Microbiol.* 73 (4), 1341–1348. doi: 10.1128/aem.02073-06

Snelgrove, P. V. R., Soetaert, K., Solan, M., Thrush, S., Wei, C.-L., and Danovaro, R. (2018). Global carbon cycling on a heterogeneous seafloor. *Trends Ecol. Evol.* 33 (2), 96–105. doi: 10.1016/j.tree.2017.11.004

Solorzano, L. (1969). Determination of ammonia in natural waters by the phenolhypochlorite method. *Limnology Oceanography* 14 (5), 799–801. doi: 10.4319/lo.1969.14.5.0799

Thamdrup, B., Fossing, H., and Jørgensen, B. B. (1994). Manganese, iron and sulfur cycling in a coastal marine sediment, Aarhus bay, Denmark. *Geochimica Cosmochimica Acta* 58 (23), 5115–5129. doi: 10.1016/0016-7037(94)90298-4

Timmermann, K., Banta, G. T., and Glud, R. N. (2006). Linking arenicola marina irrigation behavior to oxygen transport and dynamics in sandy sediments. *J. Mar. Res.* 64 (6), 915–938. doi: 10.1357/002224006779698378

Volkenborn, N., Polerecky, L., Wethey, D. S., and Woodin, S. (2010). Oscillatory porewater bioadvection in marine sediments induced by hydraulic activities of arenicola marina. *Limnology Oceanography* 55 (3), 1231–1247. doi: 10.4319/lo.2010.55.3.1231

Waldbusser, G. G., and Marinelli, R. L. (2009). Evidence of infaunal effects on porewater advection and biogeochemistry in permeable sediments: a proposed infaunal functional group framework. *J. Mar. Res.* 67, 503–532. doi: 10.1357/002224009790741120

Ward, N. D., Megonigal, J. P., Bond-Lamberty, B., Bailey, V. L., Butman, D., and Canuel, E. A. (2020). Representing the function and sensitivity of coastal interfaces in earth system models. *Nat. Commun.* 11 (1), 2458. doi: 10.1038/s41467-020-16236-2

Wilde, S., and Plante, C. (2002). Spatial heterogeneity of bacterial assemblages in marine sediments: the influence of deposit feeding byBalanoglossus aurantiacus. *Estuarine Coast. Shelf Sci.* 55 (1), 97–107. doi: 10.1006/ecss.2001.0889

Woodin, S. A. (1977). Algal "gardening" behavior by nereid polychaetes: effects on soft-bottom community structure. *Mar. Biol.* 44, 39–42. doi: 10.1007/BF00386902